PCCP

PAPER

Cite this: *Phys. Chem. Chem. Phys.*, 2018, **20**, 9343

Cell–cell bioelectrical interactions and local heterogeneities in genetic networks: a model for the stabilization of single-cell states and multicellular oscillations

Javier Cervera, * José A. Manzanares and Salvador Mafe

Received 1st December 2017,
Accepted 4th March 2018

DOI: 10.1039/c8cp00648b

rsc.li/pccp

Genetic networks operate in the presence of local heterogeneities in single-cell transcription and translation rates. Bioelectrical networks and spatio-temporal maps of cell electric potentials can influence multicellular ensembles. Could cell–cell bioelectrical interactions mediated by intercellular gap junctions contribute to the stabilization of multicellular states against local genetic heterogeneities? We theoretically analyze this question on the basis of two well-established experimental facts: (i) the membrane potential is a reliable read-out of the single-cell electrical state and (ii) when the cells are coupled together, their individual cell potentials can be influenced by ensemble-averaged electrical potentials. We propose a minimal biophysical model for the coupling between genetic and bioelectrical networks that associates the local changes occurring in the transcription and translation rates of an ion channel protein with abnormally low (depolarized) cell potentials. We then analyze the conditions under which the depolarization of a small region (patch) in a multicellular ensemble can be reverted by its bioelectrical coupling with the (normally polarized) neighboring cells. We show also that the coupling between genetic and bioelectric networks of non-excitable cells, modulated by average electric potentials at the multicellular ensemble level, can produce oscillatory phenomena. The simulations show the importance of single-cell potentials characteristic of polarized and depolarized states, the relative sizes of the abnormally polarized patch and the rest of the normally polarized ensemble, and intercellular coupling.

1. Introduction

The interplay between chemical and electrical signals contributes to the biological organization over multiple spatio-temporal scales.[1–12] Genetic and bioelectric networks are closely interrelated because the local concentrations of signalling ions (*e.g.*, calcium) and molecules (*e.g.*, serotonin and butyrate) that regulate transcriptional, translational, and post-translational processes can be influenced by the distribution of electric potential over multicellular ensembles.[2,7,12] The spatio-temporal map of cell potentials regulated by intercellular connectivity can then be relevant to the gene expression patterns of embryogenesis, regeneration and tumorigenesis.[2,7,13] The understanding of these processes requires conceptual frameworks that incorporate not only single-cell characteristics but also cell–cell interactions.

Molecular bioelectricity is emerging as an important field because of the possibility of combining bioelectrical (cell membrane potentials) and molecular biology (the specific ion channel proteins regulating these potentials) concepts. We have recently proposed a highly simplified biophysical model for the interplay between bioelectrical and genetic networks in non-excitable cells, from the local single-cell level to the long-range multicellular ensemble, and applied it to different case studies.[10,11] We explore here two new and important questions: (i) could cell–cell interactions, mediated by intercellular gap junctions, contribute to the stabilization of bioelectrical states against local heterogeneities in genetic networks? And (ii) could the coupling between bioelectric and genetic networks sustain multicellular oscillations between abnormally low (depolarized) and normal (polarized) cell potential states? To this end, we assume that significant spatial heterogeneities occur in the transcription and translation rates of an ion channel protein, analyzing the consequences of this assumption.

The first problem (i) has clear experimental interest because endogenous bioelectrical fields and signals are crucial for investigation of the morphology of organisms and tumor development in model animals.[2,8,9,14,15] In view of the role of intercellular interactions in tissue organization,[16] the above problem may also provide some biophysical insights into the mechanisms that keep cells in tissues behave normally despite local mutations,[17] the role of the microenvironment in restraining

Dept. Termodinàmica, Fac. Física, Universitat de València, 46100 Burjassot, Spain. E-mail: javier.cervera@uv.es

cancer progression,[18] and the possibility of using stochastic gene expression stabilization as a therapeutic strategy.[19] The model employed considers that cells are coupled together in multicellular ensembles and then their individual properties should be influenced by ensemble-averaged bioelectrical magnitudes.[10] These magnitudes depend on the specific protein ion channels that regulate the cell membrane potential.[20] Experimentally, ion channels and membrane potentials are involved in tumor initiation and progression.[9,21–24]

The second problem (ii) is also relevant because information processing in biological systems makes use of bioelectrical oscillatory patterns. For instance, low frequency current noise and membrane potential oscillations have been detected in glioma cells where specific K^+ and Na^+ channels can coordinate electric responses in the picoampere-range throughout large cell populations.[25] Cell membrane potentials and metabolic oscillations are also closely connected in bacterial communities at the long-range level.[26] Intercellular communication is also based on K^+ ion-channels and extracellular concentrations.[26] In particular, two biofilm communities undergoing metabolic oscillations can be coupled through electrical signaling in order to synchronize their growth dynamics.[27] In addition to the above cases concerning the interplay between bioelectrical and biochemical processes, the oscillations between polarized and depolarized cell potentials can be coupled with specific genetic pathways in the development of the two sides of an embryo.[28] Bistability and oscillatory phenomena can also arise from the coupling between voltage pulses and gene expression in excitable single-neuron models.[29] Finally, it has been shown that the gap junction-mediated electrical coupling between β-cells coordinates biochemical oscillations in pancreatic islets.[30]

A Systems Biology approach to the problem can be developed on the basis of Nonlinear Dynamics models for multicellular ensembles[31] making use of fundamental concepts explained previously.[10] We show first that local changes in the genetic network characteristics that occur over a small region (patch) of a multicellular ensemble lead to low concentrations of the protein ion channel and then to abnormally low (depolarized) cell potentials. We consider then cell–cell interactions as stabilizing agents and analyze the conditions under which this local depolarization can be reverted by the (normally polarized) neighboring cells. The bioelectrical stabilization of the whole ensemble depends on the membrane potentials of the single-cell polarized and depolarized states, the spatial extension of the abnormally polarized patch, and intercellular coupling. The simulations suggest that external actions on ensemble-averaged magnitudes such as electric potentials may influence the multicellular states that emerge from the combination of single-cell states, in agreement with recent experimental and theoretical studies.[2,7,10,31–34] Consistent with this view, we will focus here on the intercellular transfer of information in bioelectrically coupled multicellular domains rather than on the established mechanisms to control and modify single-cell states based on biochemical extracellular actions.

2. Model genetic and bioelectric networks

The membrane potential $V < 0$ is the electrical potential of the cell cytoplasm with respect to that of the extracellular environment under conditions of zero total current.[32] This magnitude characterizes the cell bioelectrical state[8,9,14,22] and is determined by the conductances of a small number of ion channels in the cell membrane together with the intracellular and extracellular ionic concentrations.[8,9,14,22,35–38] A minimal model including two opposite polarizing (pol) and depolarizing (dep) voltage-gated channels that promote high and low values of $|V|$, respectively, and allow a qualitative description of the basic experimental trends.[35,37,38] Experimentally, the hyperpolarizing *Kir2.1* and the depolarizing *Nav1.5* channels can be used for this purpose.[35]

Bioelectricity influences the spatial distribution of the signaling ions and molecules that participate in the genetic and epigenetic networks of transcriptional and translational control.[2,7,10,12,14,34] It can also act post-translationally by activating voltage-gated channels and by blocking the channels with specific ions and molecules.[15,20,32,39,40] The consequence of this complex interplay is that the kinetic equations describing the intracellular concentrations of mRNA (m) and the protein ion channel (p) must be coupled with the cell electric potentials.[10,11] In particular, we have considered that the concentration p of the protein forming the polarizing voltage-gated channel is modulated by the cell potential V (Fig. 1, bottom).[41–45]

The typical ionic concentrations are in the range 10–500 mM. For most physiological conditions[37,45] the inside and outside concentrations of the cell are almost constant and then the changes in the membrane potential are mainly due to modifications in the conductance and permeability of the relevant ion channels (opening/closing processes), as it is assumed in Fig. 1. Note that the number of ions to be transferred across the membrane in order to set up typical potential differences is very small compared with the total number of ions in the cell volume.[45] Thus, assuming the constancy of ionic concentrations is an approximately valid assumption in electrophysiological measurements concerning membrane potentials.[45] It is remarkable that embryonic and tumor (proliferative) cells are relatively depolarized and show low membrane potentials compared with terminally differentiated quiescent cells.[4,5,9,12]

The potential V given in Fig. 1 results from the condition of zero current between the cell cytoplasm and the external microenvironment, $I_{pol} + I_{dep} = 0$.[20,32] Note that Fig. 1 shows an isolated cell and then the equation for V is written under the zero current conditions that should eventually be reached. In this case, the single-cell potential coincides with the usual resting potential. The equations for the potential-dependent polarizing and depolarizing currents I_{pol} and I_{dep} (Fig. 1) show the qualitative trends observed experimentally using a minimum number of phenomenological parameters, such as the number of effective charges $z = 3$ involved in channel gating and the channel threshold potentials $V_{th,pol} = V_{th,dep} = -V_T$, where $V_T = RT/F = 27$ mV is the thermal potential, R is the gas

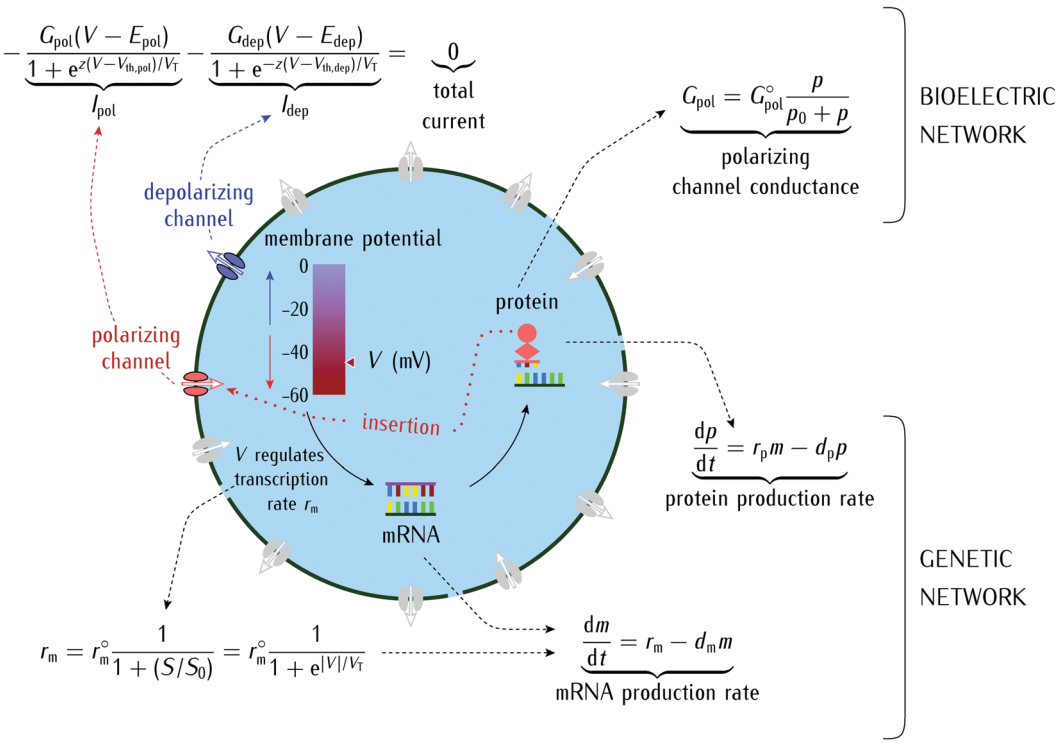

Fig. 1 The genetic and bioelectrical networks are coupled at the single-cell level. For simplicity, we consider only the transcription and translation time (t)-dependent kinetic equations for the mRNA and protein that form the polarizing channel. The genetic network (bottom, right) is based on the central dogma that describes the information flow from DNA to mRNA (transcription) to protein (translation). The channel protein concentration p is then regulated by a specific mRNA of concentration m, where m and p are relative concentrations defined with reference to the values characteristic of the particular biochemical problem studied.[10,11,41] The rate constants for mRNA transcription (r°_m) and protein translation (r_p), as well as their degradation rate constants (d_m and d_p), are difficult to estimate because these kinetic steps are governed by multiple factors[10,11,41–43] and, in particular, by the concentration S of signalling ions (bottom, left). Molecular diffusion in the cell is usually fast compared with genetic processes and can be ignored as a first approximation.[44] We assume the Hill kinetics $G_{pol}=G^{\circ}_{pol}[p/(p_0+p)]$ for the dependence of the channel conductance on the protein intracellular concentration p, where G°_{pol} is the maximum conductance and p_0 corresponds to $G^{\circ}_{pol}/2$ (top, right). The membrane potential V (vertical scale) is obtained from the condition of zero total current (top, left) and is regulated by the polarizing (G_{pol}) and depolarizing (G_{dep}) conductances. This potential depends also on the assumed equilibrium potentials E_{pol} = −60 mV and E_{dep} = 0 mV which do not change with time if the intracellular and extracellular ionic concentrations are approximately constant.[37,45]

constant, T = 310 K is the temperature and F is the Faraday constant.[20,32,37] The relative contributions of the depolarizing and polarizing channels to the total membrane conductance regulate the cell electrical state. In particular, low values of the conductance ratio G_{pol}/G_{dep} can decouple V from the normal polarized value E_{pol} to give depolarized potentials close to E_{dep}.[10,32]

The model in Fig. 1 reveals the fact that the concentration S of the signaling ion that influences the genetic rates should depend on the cell potential V.[2,3,8,34,46–50] Some experimental examples are the calcium cell entry and subsequent regulation of crucial biochemical pathways,[46–49] *e.g.* by means of a calcium-activated transcription factor,[50] and the transference of charged signaling molecules (*e.g.*, serotonin and butyrate) to the cell.[2,8] These processes are influenced by the potential difference between the intracellular and extracellular solutions. As a first approximation to this complex problem, we assume the Hill kinetics $r_m=r^{\circ}_m/[1+(S/S_0)]=r^{\circ}_m/(1+e^{|V|/V_T})$ for the transcription rate,[10] where S_0 is a reference concentration and r°_m is the transcription rate in the absence of signaling ions. Note that we consider here the case of potential-dependent negative regulation of the protein:[10] an increase in the absolute value of the potential V decreases the production of mRNA and the protein, as clearly shown by the genetic network (Fig. 1, bottom). The consequence of this interplay between the bioelectric and genetic networks of Fig. 1 is that the cell potential V modulates the concentration p of the protein forming the polarizing channel of conductance G_{pol} (Fig. 1, bottom) and, in turn, this conductance makes a significant contribution to the total membrane conductance that regulates the potential V (Fig. 1, top).

Fig. 2 shows two model cells connected by intercellular protein gap junctions that permit the transference of electric currents[10,32] and signaling molecules.[11] In this case, the cell is not isolated and then the zero current conditions of Fig. 1 are no longer valid. Instead, the potential V_i of cell i is dynamically evolving under the non-zero single-cell and gap-junction currents. The cell state of Fig. 1 can then be modulated at the ensemble level due to coupling with the neighboring cells.[10,32–34,51] Note that every individual cell i experiences the average electric potential created by its nearest-neighbor cells,

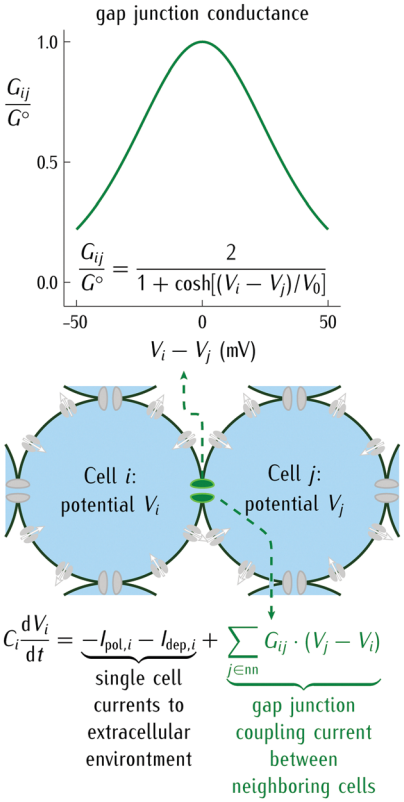

Fig. 2 The intercellular coupling allows extending the interplay between the bioelectric and genetic networks from the single-cell of Fig. 1 to the whole multicellular ensemble. The cells i and j are bioelectrically coupled by an intercellular gap junction of effective conductance G_{ij} (bottom). This conductance shows bell-shaped dependence on the potential difference $V_i - V_j$ between cells i and j (top).[10,54–56] The potential V_0 determines the width of the distribution of experimental conductances G_{ij}. The cell potential V_i changes with time t according with the intercellular current, regulated by G_{ij} and $V_i - V_j$, and the single-cell currents $I_{pol,i}$ and $I_{dep,i}$ (Fig. 1). Note that the sum over $j \in$ nn makes reference to the nearest neighbors (nn) cells.[10]

as clearly shown by the sum $\sum_{j\in nn} G_{ij}(V_j - V_i)$ in Fig. 2 where each neighbor cell potential j is weighed by the respective junction conductance G_{ij}. It is in this biophysical sense that we use the term ensemble-averaged electric potential here. In a distinct context, different expressions to define synaptic gap-junction currents in theoretical models of coupled excitable cells have been proposed.[52,53] In our case, we have used the bell-shaped function shown in Fig. 2 because it captures most of the experimental trends observed in the voltage-gating of connexin proteins in vertebrate junctions;[54–56] see, in particular, Fig. 2 and Table 1 of ref. 56 for a comprehensive experimental account.

To better show the qualitative characteristics of intercellular coupling, we consider the conductance ratios G°_{pol}/G_{dep} and G°/G_{dep} that describe the relative contributions of the single-cell (G°_{pol}) and intercellular (G°) effective conductances with respect to G_{dep}, where G° is the maximum conductance of the gap junction (Fig. 2). Large intercellular conductances favor isopotential multicellular ensembles while low conductances would give essentially isolated cells with no electrical communication. Autonomous cell behavior due to abnormal intercellular communication may be involved in the initial states of tumorigenesis.[16,54,55]

Genetic networks operate in the presence of local heterogeneities in the single-cell transcription and translation rates. In particular, we analyze local heterogeneities in the genetic rate constants of Fig. 1. To this end, we assume that a patch formed by a small number N_2 of cells shows values of r°_m and r_p that are significantly different from the rest of the cells in an ensemble with $N = 1112$ cells. The locally-different genetic rates eventually give distinct cell bioelectrical states that are shown in the current–voltage (I–V) curves of the cells in the bulk of the ensemble (1) and in the patch (2).

Initially, all cells in the ensemble have the same potential $V_i(t = 0)$, $i = 1,\ldots,N$. The initial concentrations of mRNA and proteins are calculated by solving the kinetic equations given in Fig. 1 under steady-state conditions.[10] For $t > 0$, the time evolution of the system is obtained by solving the N equations for $V_i(t)$ of Fig. 2. Ref. 10 and 32 describe the numerical algorithms used. The system shows an electrical relaxation time electrical time $C_i/G_{pol}{}^\circ$ lower than 1 s for cell capacitances in the range C_i = 10–100 pF and conductances in the range $G^\circ_{pol} = 0.1-1$ nS.[10,32,33,57] In contrast, the time response characteristic of the genetic network is relatively slow. For instance, transcription and translation rate constants in the range 0.1–1 min^{-1} give times between 1 and 10 min while degradation rate constants in the range 0.003–0.1 min^{-1} give times between 0.1 and 5 h.[10,11,42]

3. Results and discussion

3.1 Stabilization of multicellular states against local genetic heterogeneities

The simulations given in Fig. 3 consider a spatial heterogeneity in the genetic rates r°_m and r_p that are assumed to decrease in the patch of N_2 cells with respect to the values prevailing over the rest of the multicellular ensemble. The local differences in the genetic rates of Fig. 3 produce a spatial regionalization of the polarizing channel expression (Fig. 1) that eventually results in distinct current–voltage (I–V) responses for the cells in the patch and in the bulk of the ensemble (Fig. 3, top, right). These curves are obtained using the model in Fig. 1 under steady-state conditions and show the effect of decreasing the genetic rates characteristic of the polarizing channel protein in the patch. The cells in this patch have only one stable depolarized potential (curve 2) while the rest of the cells have two stable polarized (high $|V|$) and depolarized (low $|V|$) potentials (curve 1).

Initially ($t = 0$), all cells in the multicellular ensemble have the same electrical state: the stable polarized potential (curve 1) that characterizes the normal cell state. However, the polarized potential is not stable for the cells in the patch (curve 2) because their genetic rates r°_m and r_p are assumed to decrease with respect to those in the rest of the ensemble at $t = 0$. Hence, these cells will tend to evolve towards their stable depolarized

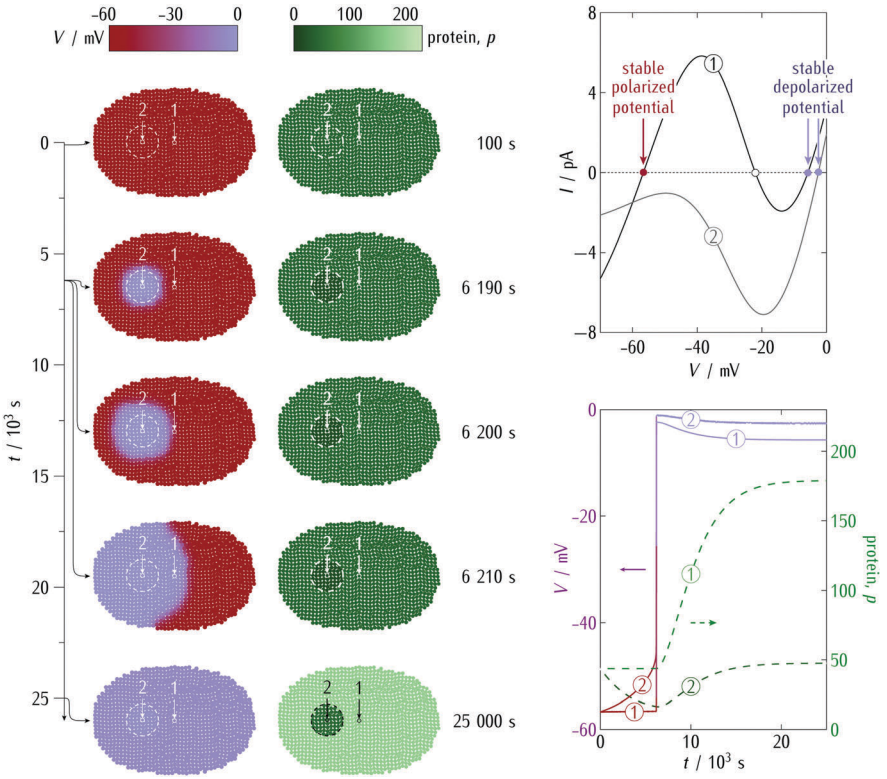

Fig. 3 The cell potential and protein concentration spatio-temporal maps (left) are obtained using the models in Fig. 1 and 2 for the case of a patch formed by $N_2 \approx 62$ cells with a spatial heterogeneity in the genetic rate constants. The polarizing channel transcription and translation rate constants are $r_m^\circ = 0.5\ \mathrm{min}^{-1}$ and $r_p = 0.5\ \mathrm{min}^{-1}$. At $t = 0$, these rate constants are decreased to $r_m^\circ = 0.25\ \mathrm{min}^{-1}$ and $r_p = 0.25\ \mathrm{min}^{-1}$ in the patch, which gives a local depolarization. The degradation rate constants are $d_m = 0.025\ \mathrm{min}^{-1}$ and $d_p = 0.025\ \mathrm{min}^{-1}$. The protein concentration $p_0 = 60$ and the conductance ratio is $G_{pol}^\circ / G_{dep} = 1.5$.[10,32] The coupling gap junction conductances are relatively high ($G^\circ/G_{dep} = 0.5$ and $V_0 = 18$ mV) over the strongly-connected multicellular ensemble. The current–voltage (I–V) curves with the stable polarized (curve 1) and depolarized (curves 1 and 2) cell potentials (top, right) together with the time evolution of the protein concentration and cell potential (bottom, right) are shown for cell 1 in the bulk of the ensemble and cell 2 inside the patch.

potential (curve 2) which is consistent with their locally different genetic rates. This abnormally low potential is characteristic of the abnormal cell state resulting from the local decrease in the genetic rate constants.

Fig. 3 shows the spatio-temporal maps of cell potentials and protein concentrations over a strongly-connected multicellular ensemble. The depolarized potential is a stable state for all cells in the ensemble (curves 1 and 2) and, eventually, the intercellular coupling makes the whole ensemble attain the depolarized value of $|V|$ (Fig. 1 and 2). Fig. 3 shows also the time evolution of the protein concentration p and the potential V for a cell 1 in the bulk of the ensemble and another cell 2 inside the patch. Depolarization cannot be avoided by the increase of the polarizing channel protein concentration in cells 1 and 2 (Fig. 3, right) that occurs after depolarization because of the negative regulation of the electric potential $|V|$ on the concentration p (Fig. 1).

Fig. 4 considers the opposite case of a weakly connected multicellular ensemble where the parameter that determines the width of the gap junction conductance distribution has been decreased to $V_0 = 13.5$ mV while keeping $G^\circ/G_{dep} = 0.5$ constant (Fig. 2). Because of the weak intercellular coupling (Fig. 4, right), depolarization cannot proceed through the whole ensemble and is now confined to the patch, which becomes electrically isolated (Fig. 4, left). As in the case of embryogenesis where the locally different genetic expression of ion pumps and channels can result in bioelectrical regionalisations,[3,8,15,58] the existence of spatially heterogeneous cell polarizations immediately suggests weakly-connected multicellular ensembles. Note also the correspondence between the constant values of potential V and concentration p in cell 1 of the polarized part of the ensemble (Fig. 4, right). As for cell 2, the protein concentration p decreases first because of the decreased genetic rates and increases later because of the low values of $|V|$ characteristic of depolarization and the potential-dependent negative regulation of the protein assumed in Fig. 1 (see also Fig. 3 for a similar effect).

When the patch size is small enough, its depolarization can be avoided even when the local genetic rates may favor it (Fig. 5, left; compare Fig. 5 with Fig. 3). This bioelectrical stabilization occurs only when intercellular coupling is sufficiently strong and the number of cells in the patch size is low (Fig. 5, top, right). The transition between the polarized and depolarized stable states of cell 2 is abrupt because of the potential bistability of the I–V curve (Fig. 3, top, right), suggesting that the

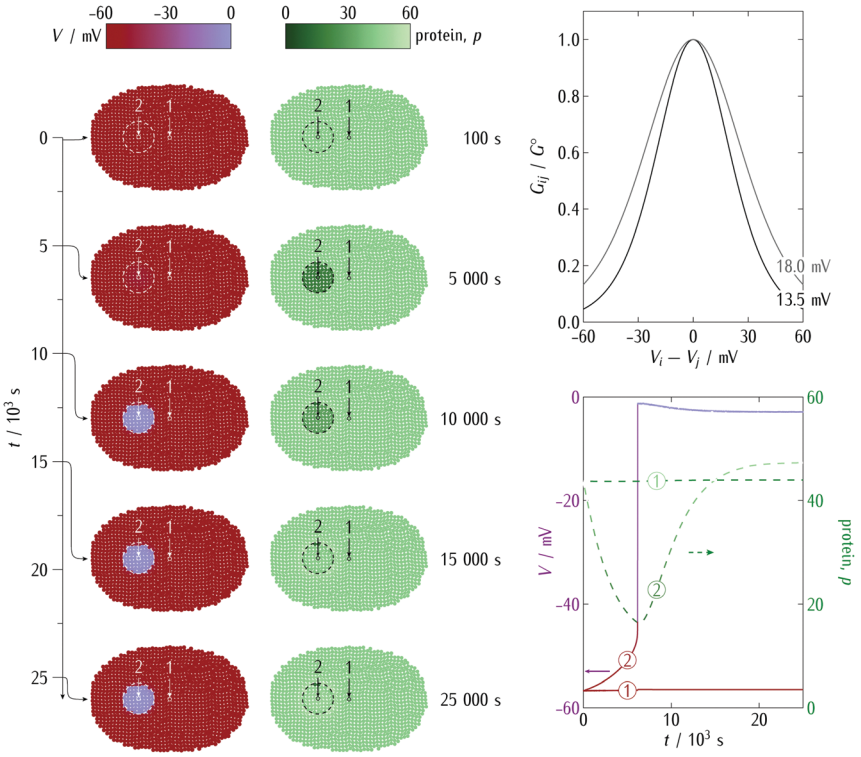

Fig. 4 The cell potential and protein concentration spatio-temporal maps (left) obtained under the same conditions of Fig. 3 except for the width of the bell-shaped gap junction conductance which is narrower than that in Fig. 3 because now V_0 = 13.5 mV instead of V_0 = 18 mV (top, right). The lower value of V_0 decreases the intercellular coupling provided by the junction conductance and avoids then the depolarization of the whole ensemble obtained in Fig. 3 for the case of a strongly-connected ensemble.

number of cells in the patch can be critical to avoid depolarization (Fig. 5, top, right). In this case, the potential of cell 2 decreases in the absolute value but this slight depolarization is not enough for the potential-dependent negative regulation shown in Fig. 1 to compensate for the decrease in the genetic rates. Hence, the polarizing channel concentration p decreases (Fig. 5, bottom, right). However, cell 2 can still resist depolarization because of the strong coupling with the multicellular ensemble that acts now as a bioelectrical buffer.

3.2 Bioelectrical oscillations in multicellular ensembles

Fig. 6 considers again the case of Fig. 3 but now the transcription and translation rate constants are maintained at 0.25 min^{-1} in the patch while they are increased to 1 min^{-1} in the rest of the ensemble. As a consequence, the cells in the rest of the ensemble have only one stable polarized potential in the I–V curve (Fig. 6, top, right) rather than the two stable (polarized and depolarized) values obtained in the case of Fig. 3 (curve 1). This fact causes most of the cells in the ensemble to have only one stable (polarized) value of $|V|$ in the I–V curve 1 (Fig. 6, top, right) rather than the two stable (polarized and depolarized) values obtained in the case of Fig. 3. As in the case of Fig. 3, however, the only stable value of $|V|$ in curve 2 is depolarized (Fig. 6, top, right). These unique and opposite stable states for the cells in the patch and its neighborhood, together with the negative regulation between the protein concentration and the cell potential (Fig. 1), cause oscillations between the polarized and depolarized states of the cells in the patch (Fig. 6, left) that involve a time scale much longer than the electrical relaxation time.

Note also that the bi-stability of the I–V curves (Fig. 3–6) results in sharp responses that might be smoothed in real experimental systems where the difference between the polarized and depolarized cell states could not be so marked because of the high number of channels involved.[22,38,58,59] Also, we have implicitly assumed rapid distribution equilibria for the concentration of signaling ions that regulate transcription shown in Fig. 1 and 2 and ignored their slow electrodiffusion over the multicellular ensemble.

It has been suggested that information processing in biological systems can make use of oscillatory patterns. For instance, coupled oscillations of polarized and depolarized cell potentials can occur on the two sides of an embryo.[28] Also, oscillatory phenomena and bistability may result from the interplay between voltage pulses and gene expression in excitable single-neuron models.[43] In the case of Fig. 6, however, the oscillations arise from the dynamics of the individual genetic and bioelectric networks of non-excitable cells which are coupled by average electric potentials at the multicellular ensemble level, without assuming any periodic time dependence of the single-cell biological magnitudes. Note that the oscillations of Fig. 6 could not be observed in Fig. 3 because in the latter case the majority of the cellular ensemble had also one stable depolarized state in addition to the polarized state (see the I–V curve of Fig. 3). Weak intercellular coupling would

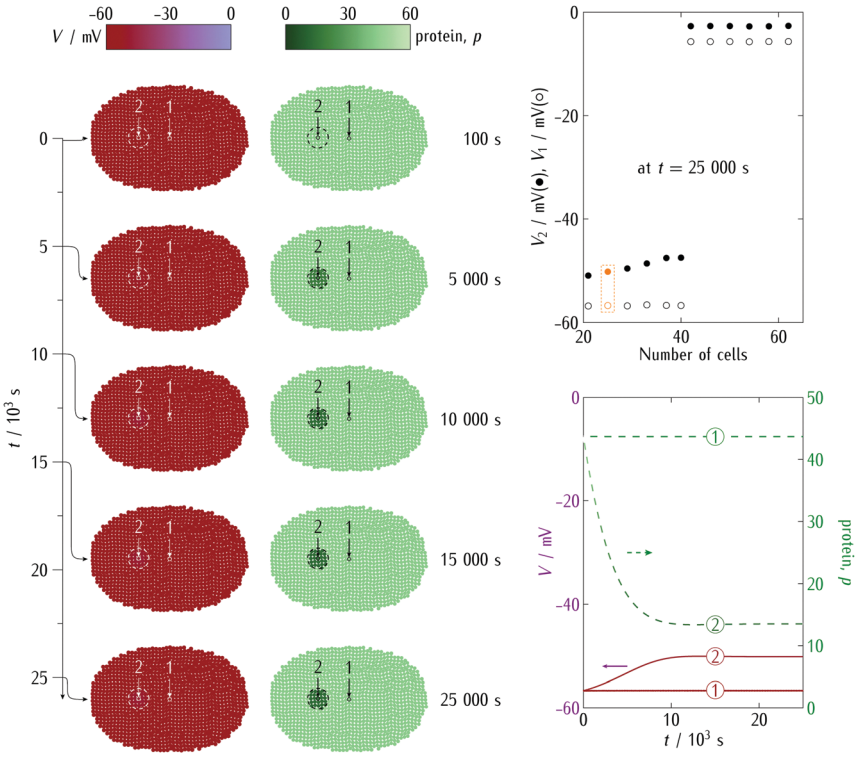

Fig. 5 The cell potential and protein concentration spatio-temporal maps (left) are obtained under the same conditions as in Fig. 3 except for the patch size, which is now decreased to $N_2 \approx 25$ cells with respect to that of Fig. 3 ($N_2 \approx 62$). The strong coupling with the polarized cells in the rest of the ensemble provides bioelectrical stabilization against the local decrease in the genetic rate constants that strive for depolarization (Fig. 3). Note the sharp transition between the polarized and depolarized stable potentials of cells 1 and 2 at $N_2 \approx 42$ (top, right). Compare also the time evolutions of the protein concentrations and cell potentials (bottom, right) with those of Fig. 3.

prevent the surrounding cells to repolarize the patch (Fig. 4) making the oscillation difficult. In Fig. 5, the small patch could hardly resist the stabilization forced by the rest of the cells and thus significant depolarization would not be possible.

In order to better determine the conditions that allow oscillatory phenomena, Fig. 7 shows the effect of the number of cells N_2 in the patch at fixed intercellular connectivity and Fig. 8 shows the effect of intercellular connectivity at fixed number N_2. At time $t = 0$ the cells in the ensemble show the same polarized potential (Fig. 7) that characterizes the normal cell state.[10,11] This polarized potential is stable except for those cells in the patch, which have relatively low values of the rates r_m° and r_p shown in Fig. 7 and 8 with respect to the rest of the ensemble. These decreased production rates eventually give low values of the polarizing channel protein. Therefore, the cells in the patch tend to the stable depolarized potential state consistent with the locally different genetic rates assumed. However, because of the stabilizing effect exerted by the majority of polarized cells in the ensemble over the minority of depolarized cells in the patch, this transition from the polarized to the depolarized state is only possible for a large patch (Fig. 7, top) but not for the small one, even for low protein concentrations (Fig. 7, bottom). In between these extreme cases, the oscillations of the cells in the patch can be sustained by the interplay between the genetic (protein concentration of Fig. 7, right) and electric (cell potential of Fig. 7, left) networks.

Fig. 8 considers the case of Fig. 7 but now the number of cells in the small patch is kept constant and it is the intercellular connectivity, described by the dimensionless gap junction maximum conductance G°/G_{dep} (see Fig. 2) that is changed. This case is also of experimental interest: weakly-connected multicellular ensembles should give spatial heterogeneities of cell polarization that can play a role in embryogenesis where the local expression of ion pumps and channels leads to regionalization.[7,15,58] In contrast, an essentially isopotential ensemble where no patterning information could be stored should result for strongly-connected ensembles.[10] In this case, the strong coupling with the majority of cells in the rest of the ensemble would provide bioelectrical stabilization of the small patch against local fluctuations of the genetic rates, avoiding the autonomous behavior of the patch.[7,10] Interestingly when the patch is sufficiently large, abnormally depolarized states cannot be reverted (Fig. 7, top).

Fig. 8 shows that oscillations are possible only over a range of intermediate intercellular connectivities. Indeed, when the intercellular coupling characterized by G°/G_{dep} is sufficiently strong, the patch remains in the polarized state enforced by the rest of the ensemble (Fig. 8, bottom). In contrast, when the coupling is too weak, the patch eventually reaches the depolarized stable state (Fig. 8, top), being now electrically isolated from the rest of the ensemble. Hence, changing the coupling provided by the intercellular gap junctions allows the flexible

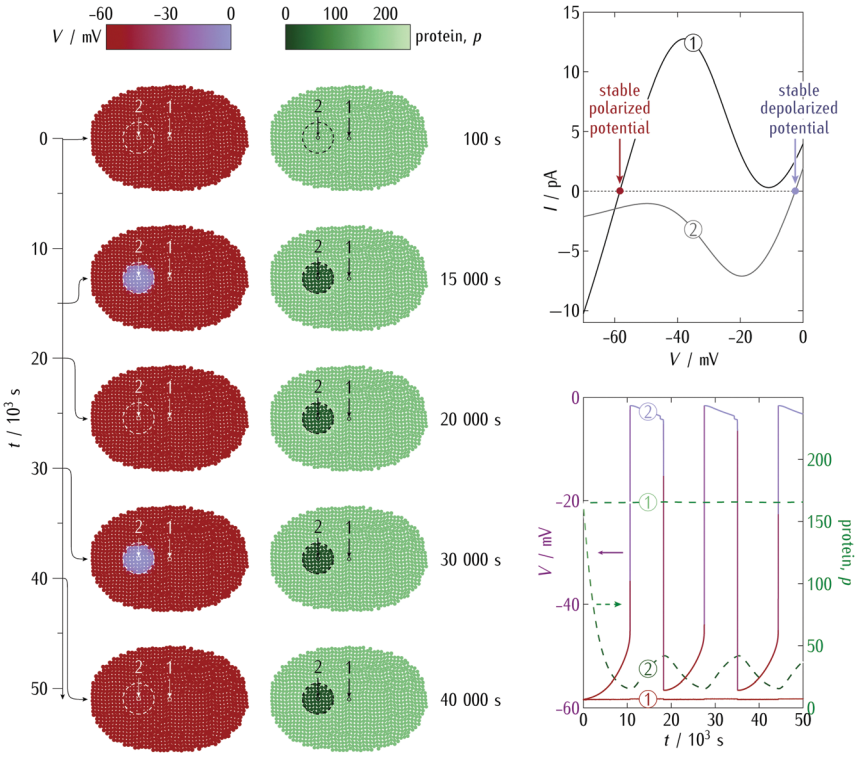

Fig. 6 The cell potential and protein concentration spatio-temporal maps (left) are obtained under the same conditions as in Fig. 3 except for the transcription and translation rate constants outside the patch, which are now increased to $r_m^\circ = 1\ \mathrm{min}^{-1}$ and $r_p = 1\ \mathrm{min}^{-1}$. This increase in the genetic rates causes the steady state I–V curve of the cells in the patch (top, right) to have only one stable polarized potential (curve 1), as opposed to the unique depolarized potential characteristic of the cells in the patch (bottom, right). These unique and opposite stable states can sustain local oscillations between the polarized and the depolarized states in the patch (bottom, right).

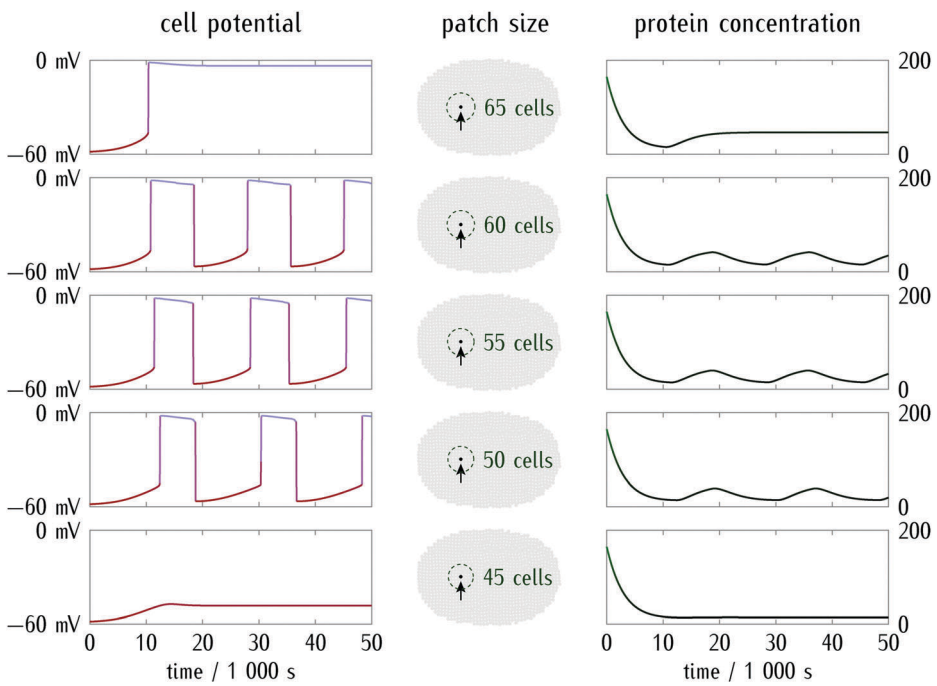

Fig. 7 The oscillations of the cell potential (left) and protein concentration (right) for a cell at the center of the small patch as a function of time t, from t = 10 s to 50 000 s, for different numbers of cells in the patch. All cells in the ensemble are characterized by the values shown in Fig. 1, with the intercellular coupling parameters $G^\circ/G_{dep} = 0.5$ and $V_0 = 18$ mV (see Fig. 2). The genetic network of Fig. 1 operates with a spatial heterogeneity in the rate constants: the cells outside the patch have the rates $r_m^\circ = 1\ \mathrm{min}^{-1}$ and $r_p = 1\ \mathrm{min}^{-1}$ while these rates are decreased to $r_m^\circ = 0.25\ \mathrm{min}^{-1}$ and $r_p = 0.25\ \mathrm{min}^{-1}$ for those cells in the patch. The degradation rate constants are those in Fig. 3 all over the ensemble. The initial conditions (t = 0) correspond to the steady-state solution for the polarized state of the cells outside the patch.

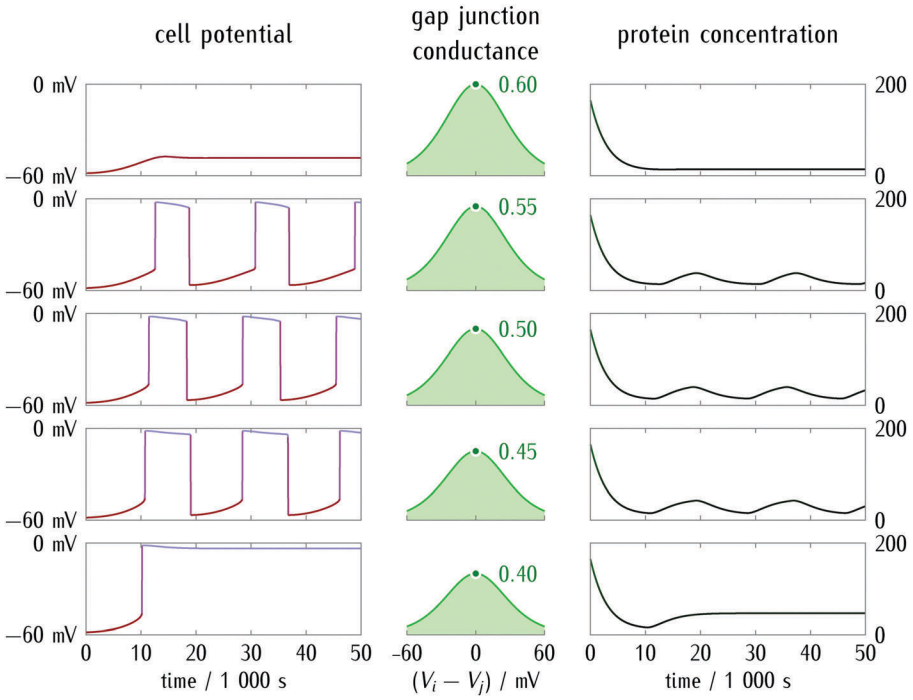

Fig. 8 The oscillations of the cell potential (left) and protein concentration (right) for a cell at the center of the small patch as a function of time t. The curves are now obtained for different values of the dimensionless gap junction maximum conductance G°/G_{dep} describing the intercellular connectivity in the patch and a fixed number of cells $N_2 = 55$. The other conditions and parameters are the same as in Fig. 7. Note the regimes of weak (bottom curves) and strong (top curves) coupling. In the first case, the cells in the patch are essentially isolated from the rest of the ensemble and remain then depolarized. In the second case, these cells are stabilized by the majority of surrounding polarized cells despite of the locally low rate constants of the patch favoring depolarization (Fig. 7).

topology which is needed to establish/abolish bioelectrical oscillations. Note that the oscillations in Fig. 7 and 8 are not centrally organized and arise when the individual genetic and bioelectric networks of every non-excitable cell are coupled at the multicellular level. Indeed, average electric potentials make the cells in the patch act as an oscillating multicellular aggregate. This fact is clearly shown by the gradual reduction observed in the residence time of the depolarized cell state when the number of interacting cells in the oscillating patch is decreased (Fig. 7, left).

Taken together, Fig. 3–8 suggest that bioelectrical effects may contribute to the normalization and stabilization of multicellular states in the presence of spatial heterogeneities in the transcription and translation rates of an ion channel protein. In particular, we have established the conditions under which the local depolarization of a small patch with abnormally low cell potentials could be avoided by intercellular coupling with the normally polarized multicellular ensemble. In addition, Fig. 3–8 show that the combined action of genetic pre-patterns with intercellular coupling can give a variety of dynamic responses, which are coded in the spatio-temporal maps of electric potentials,[10,34] as suggested experimentally in model animals.[49] These responses are based on collective phenomena (Fig. 2) that cannot be deduced directly from the individual cell characteristics (Fig. 3): the oscillations of Fig. 6–8, for instance, are sustained by the coupling of a small patch whose stable state is depolarized with an ensemble whose stable state is polarized.

4. Conclusions

The model considered here is too simple to be applied to real biological problems but can give useful qualitative insights into complex problems. Fig. 3–8 show that the single-cell bioelectrical state depends not only on the potential V_i (Fig. 1) but also on the potential difference $V_i - V_j$ relative to the neighboring cells j (Fig. 2). In this context, it could be possible that multicellular ensembles allowed system-level responses to local genetic changes. In the model studied here, the dynamics of the multicellular ensemble governed by the voltage-gated intercellular junctions allows the bioelectrical normalization and stabilization of patches against local changes in the genetic network (Fig. 5). However, when these patches are large, the extension of the abnormal depolarization to the whole multicellular ensemble may occur for high intercellular connectivity (Fig. 3) but not for low connectivity (Fig. 4). Therefore, the effects of intercellular connectivity depend here on the number of abnormal cells involved. Oscillations between normally and abnormally polarized cellular states can also be obtained (Fig. 6–8), which suggests that oscillatory phenomena can support information processing not only in neural networks[43] but also in non-excitable cells, as observed experimentally[28,49] and suggested theoretically[2,7] by Levin and co-workers.

Enhancing the intercellular connectivity might smooth the effects of the local genetic fluctuations that would otherwise produce abnormal cell polarizations over small patches of the

multicellular ensemble. It is tempting to speculate about this bioelectrical stabilization in relation to the intrinsically stochastic nature of single-cell genetics.[60] However, it is an experimental fact that bioelectrical effects are usually coupled with other complex and highly-specific biomechanical and biochemical pathways. For instance, cell depolarization, lipid membrane biomechanics, and biochemical networks may act together to favor cell proliferation[61] and thus more elaborated physical models are necessary.[34]

It should also be mentioned that experimental attempts to enhance intercellular coupling may produce different side effects associated with the distinct signaling molecules that could be transferred between cells, thus providing either an advantage or a disadvantage to the target cells.[54,55,62,63] In addition, procedures aimed at controlling bioelectrical states must allow a localized spatio-temporal control to avoid undesired side effects. In principle, this control could be based on conducting polymer microwires,[64] nanoparticle–cell binding,[39,65] local injection of mRNA encoding specific ion channels and forced cell polarization/depolarization *via* pharmacological and molecular genetic methods,[66] and optogenetic techniques.[67]

Conflicts of interest

There are no conflicts to declare.

Acknowledgements

We acknowledge the financial support of the Spanish Ministry of Economic Affairs and Competitiveness (MAT2015-65011-P) and European Regional Development Fund.

Notes and references

1 R. H. W. Funk and C. Thiede, Ion gradients and electric fields – an intrinsic part of biological processes, *J. Clin. Exp. Oncol.*, 2014, **S1**, 004.
2 M. Levin, Endogenous bioelectrical networks store non-genetic patterning information during development and regeneration, *J. Physiol.*, 2014, **592**, 2295–2305.
3 J. Krüger and J. Bohrmann, Bioelectric patterning during oogenesis: stage-specific distribution of membrane potentials, intracellular pH and ion-transport mechanisms in *Drosophila ovarian* follicles, *BMC Dev. Biol.*, 2015, **15**, 1.
4 S. Sundelacruz, M. Levin and D. L. Kaplan, Role of membrane potential in the regulation of cell proliferation and differentiation, *Stem Cell Rev. Rep.*, 2009, **5**, 231–246.
5 S. Sundelacruz, M. Levin and D. L. Kaplan, Depolarization alters phenotype, maintains plasticity of predifferentiated mesenchymal stem cells, *Tissue Eng., Part A*, 2013, **19**, 1889–1908.
6 C. D. McCaig, B. Song and A. M. Rajnicek, Electrical dimensions in cell science, *J. Cell Sci.*, 2009, **122**, 4267–4276.
7 J. Mathews and M. Levin, Gap junctional signaling in pattern regulation: physiological network connectivity instructs growth and form, *Dev. Neurobiol.*, 2017, **77**, 643–673.
8 V. P. Pai, S. Aw, T. Shomrat, J. M. Lemire and M. Levin, Transmembrane voltage potential controls embryonic eye patterning in *Xenopus laevis*, *Development*, 2012, **139**, 313–323.
9 B. T. Chernet and M. Levin, Transmembrane voltage potential is an essential cellular parameter for the detection and control of tumor development in a Xenopus model, *Dis. Models & Mech.*, 2013, **6**, 595–607.
10 J. Cervera, S. Meseguer and S. Mafe, The interplay between genetic and bioelectrical signaling permits a spatial regionalisation of membrane potentials in model multicellular ensembles, *Sci. Rep.*, 2016, **6**, 35201.
11 J. Cervera, S. Meseguer and S. Mafe, MicroRNA intercellular transfer and bioelectrical regulation of model multicellular ensembles by the gap junction connectivity, *J. Phys. Chem. B*, 2017, **121**, 7602–7613.
12 M. Levin, G. Pezzulo and J. M. Finkelstein, Endogenous bioelectric signaling networks: exploiting voltage gradients for control of growth and form, *Annu. Rev. Biomed. Eng.*, 2017, **19**, 353–387.
13 F. Durant, J. Morokuma, C. Fields, K. Williams, D. S. Adams and M. Levin, Long-term, stochastic editing of regenerative anatomy *via* targeting endogenous bioelectric gradients, *Biophys. J.*, 2017, **112**, 2231–2243.
14 V. P. Pai, J. M. Lemire, J. F. Paré, G. Lin, Y. Chen and M. Levin, Endogenous gradients of resting potential instructively pattern embryonic neural tissue *via* notch signaling and regulation of proliferation, *J. Neurosci.*, 2015, **35**, 4366–4385.
15 M. Emmons-Bell, F. Durant, J. Hammelman, N. Bessonov, V. Volpert, J. Morokuma, K. Pinet, D. S. Adams, A. Pietak, D. Lobo and M. Levin, Gap junctional blockade stochastically induces different species-specific head anatomies in genetically wild-type *Girardia dorotocephala* flatworms, *Int. J. Mol. Sci.*, 2015, **16**, 27865–27896.
16 A. M. Soto and C. Sonnenschein, The tissue organization field theory of cancer: a testable replacement for the somatic mutation theory, *BioEssays*, 2011, **33**, 332–340.
17 H. Rubin, What keeps cells in tissues behaving normally in the face of myriad mutations?, *BioEssays*, 2006, **28**, 515–524.
18 M. J. Bissell and W. C. Hines, Why don't we get more cancer? A proposed role of the microenvironment in restraining cancer progression, *Nat. Med.*, 2011, **17**, 320–329.
19 J.-P. Capp, Stochastic gene expression stabilization as a new therapeutic strategy for cancer, *BioEssays*, 2012, **34**, 170–173.
20 B. Hille, *Ion Channels of Excitable Membranes*, Sunderland, MA: Sinauer Associates, 2nd edn, 1992.
21 S. Berzingi, M. Newman and H.-G. Yu, Altering bioelectricity on inhibition of human breast cancer cells, *Cancer Cell Int.*, 2016, **16**, 72.
22 M. Yang and W. J. Brackenbury, Membrane potential and cancer progression, *Front. Physiol.*, 2013, **4**, 185.
23 E. Bates, Ion channels in development and cancer, *Annu. Rev. Cell Dev. Biol.*, 2015, **31**, 231–247.

24 L. Klumpp, E. C. Sezgin, F. Eckert and S. M. Huber, Ion channels in brain metastasis, *Int. J. Mol. Sci.*, 2016, **17**, 1513.

25 P. R. F. Rocha, P. Schlett, L. Schneider, M. Dröge, V. Mailänder, H. L. Gomes, P. W. M. Blom and D. M. de Leeuw, Low frequency electric current noise in glioma cell populations, *J. Mater. Chem. B*, 2015, **3**, 5035–5039.

26 A. Prindle, J. Liu, M. Asally, S. Ly, J. Garcia-Ojalvo and G. M. Süel, Ion channels enable electrical communication in bacterial communities, *Nature*, 2015, **527**, 59–63.

27 J. Liu, R. Martinez-Corral, A. Prindle, D. D. Lee, J. Larkin, M. Gabalda-Sagarra, J. Garcia-Ojalvo and G. M. Süel, Coupling between distant biofilms and emergence of nutrient time-sharing, *Science*, 2017, **356**, 638–642.

28 B. T. Chernet, C. Fields and M. Levin, Long-range gap junctional signaling controls oncogene-mediated tumorigenesis in *Xenopus laevis* embryos, *Front. Physiol.*, 2015, **5**, 519.

29 V. P. Zhdanov, Three generic bistable scenarios of the interplay of voltage pulses and gene expression in neurons, *Neural Netw.*, 2013, **44**, 51–63.

30 T. H. Hraha, M. J. Westacott, M. Pozzol, A. M. Notary, P. M. McClatchey and R. K. P. Benninger, Phase transitions in the multi-cellular regulatory behavior of pancreatic islet excitability, *PLoS Comput. Biol.*, 2014, **10**, e1003819.

31 S. Dinicola, F. D'Anselmi, A. Pasqualato, S. Proietti, E. Lisi, A. Cucina and M. Bizzarri, A systems biology approach to cancer: Fractals, attractors, and nonlinear dynamics, *OMICS*, 2011, **15**, 93–104.

32 J. Cervera, A. Alcaraz and S. Mafe, Bioelectrical signals and ion channels in the modeling of multicellular patterns and cancer biophysics, *Sci. Rep.*, 2016, **6**, 20403.

33 A. Pietak and M. Levin, Exploring instructive physiological signaling with the bioelectric tissue simulation engine, *Front. Bioeng. Biotechnol.*, 2016, **4**, 55.

34 A. Pietak and M. Levin, Bioelectric gene and reaction networks: computational modelling of genetic, biochemical and bioelectrical dynamics in pattern regulation, *J. R. Soc., Interface*, 2017, **14**, 20170425.

35 R. D. Kirkton and N. Bursac, Engineering biosynthetic excitable tissues from unexcitable cells for electrophysiological and cell therapy studies, *Nat. Commun.*, 2011, **2**, 300.

36 M. B. A. Djamgoz, Biophysics of cancer: cellular excitability ''CELEX'' hypothesis of metastasis, *J. Clin. Exp. Oncol.*, 2014, **S1**, 005.

37 J. Cervera, A. Alcaraz and S. Mafe, Membrane potential bistability in non-excitable cells as described by inward and outward voltage-gated ion channels, *J. Phys. Chem. B*, 2014, **118**, 12444–12450.

38 R. Law and M. Levin, Bioelectric memory: modeling resting potential bistability in amphibian embryos and mammalian cells, *Theor. Biol. Med. Modell.*, 2015, **12**, 22.

39 E. A. K. Warren and C. K. Payne, Cellular binding of nanoparticles disrupts the membrane potential, *RSC Adv.*, 2015, **5**, 13660–13666.

40 C. Verdiá-Báguena, M. Queralt-Martín, V. M. Aguilella and A. Alcaraz, Protein ion channels as molecular ratchets. Switchable current modulation in outer membrane protein F porin induced by millimolar La^{3+} ions, *J. Phys. Chem. C*, 2012, **116**, 6537–6542.

41 H. Bolouri and E. H. Davidson, Modeling transcriptional regulatory networks, *BioEssays*, 2002, **24**, 1118–1129.

42 V. P. Zhdanov, Kinetic models of gene expression including non-coding RNAs, *Phys. Rep.*, 2011, **500**, 1–42.

43 V. P. Zhdanov, Three generic bistable scenarios of the interplay of voltage pulses and gene expression in neurons, *Neural Netw.*, 2013, **44**, 51–63.

44 G. Tiana, S. Krishna, S. Pigolotti, M. H. Jensen and K. Sneppen, Oscillations and temporal signalling in cells, *Phys. Biol.*, 2007, **4**, R1–R17.

45 B. Alberts, A. Johnson, J. Lewis, M. Raff, K. Roberts and P. Walter, *Molecular Biology of the Cell*, Garland Science, New York, 4th edn, 2002.

46 M. Barbado, K. Fablet, M. Ronjat and M. De Waard, Gene regulation by voltage-dependent calcium channels, *Biochim. Biophys. Acta*, 2009, **1793**, 1096–1104.

47 X. Huang and L. Y. Jan, Targeting potassium channels in cancer, *J. Cell Biol.*, 2014, **206**, 151–162.

48 G. R. Monteith, D. McAndrew, H. M. Faddy and S. J. Roberts-Thomson, Calcium and cancer: targeting Ca^{2+} transport, *Nat. Rev. Cancer*, 2007, **7**, 519–530.

49 F. Durant, D. Lobo, J. Hammelman and M. Levin, Physiological controls of large-scale patterning in planarian regeneration: a molecular and computational perspective on growth and form, *Regeneration*, 2016, **3**, 78–102.

50 R. L. Calabrese, Channeling the central dogma, *Neuron*, 2014, **82**, 725–727.

51 T. R. Gowrishankar and J. C. Weaver, An approach to electrical modeling of single and multiple cells, *Proc. Natl. Acad. Sci. U. S. A.*, 2003, **100**, 3203–3208.

52 B. M. Adhikari, A. Prasad and M. Dhamala, Time-delay-induced phase-transition to synchrony in coupled bursting neurons, *Chaos*, 2011, **21**, 023116.

53 I. Belykh, E. de Lange and M. Hasler, Synchronization of bursting neurons: what matters in the network topology, *Phys. Rev. Lett.*, 2005, **94**, 188101.

54 D. Banerjee, Connexin's connection in breast cancer growth and progression, *Int. J. Cell Biol.*, 2016, 9025905.

55 M. Mesnil, S. Crespin, J. L. Avanzo and M. L. Zaidan-Dagli, Defective gap junctional intercellular communication in the carcinogenic process, *Biochim. Biophys. Acta*, 2005, **1719**, 125–145.

56 D. González, J. M. Gómez-Hernández and L. C. Barrio, Molecular basis of voltage dependence of connexin channels: an integrative appraisal, *Prog. Biophys. Mol. Biol.*, 2007, **94**, 66–106.

57 S. Baigent, J. Stark and A. Warner, Modelling the effect of gap junction nonlinearities in systems of coupled cells, *J. Theor. Biol.*, 1997, **186**, 223–239.

58 M. Levin, Reprogramming cells and tissue patterning via bioelectrical pathways: molecular mechanisms and biomedical opportunities, *Wiley Interdiscip. Rev.: Syst. Biol. Med.*, 2013, **5**, 657–676.

59 A. T. Esser, K. C. Smith, J. C. Weaver and M. Levin, Mathematical model of morphogen electrophoresis through gap junctions, *Dev. Dyn.*, 2006, **235**, 2144–2159.

60 J.-P. Capp, Stochastic gene expression, disruption of tissue averaging effects and cancer as a disease of development, *BioEssays*, 2005, **27**, 1277–1285.
61 A. Accardi, Lipids link ion channels and cancer, *Science*, 2015, **349**, 789–790.
62 L. Zong, Y. Zhu, R. Liang and H.-B. Zhao, Gap junction mediated miRNA intercellular transfer and gene regulation: a novel mechanism for intercellular genetic communication, *Sci. Rep.*, 2016, **6**, 19884.
63 T. Aasen, M. Mesnil, C. C. Naus, P. D. Lampe and D. W. Laird, Gap junctions and cancer: communicating for 50 years, *Nat. Rev. Cancer*, 2016, **16**, 775–788.
64 D. T. Jayaram, Q. Luo, S. B. Thourson, A. H. Finlay and C. K. Payne, Controlling the resting membrane potential of cells with conducting polymer microwires, *Small*, 2017, **13**, 1700789.
65 E. H. Shin, Y. Li, U. Kumar, H. V. Sureka, X. Zhang and C. K. Payne, Membrane potential mediates the cellular binding of nanoparticle, *Nanoscale*, 2013, **5**, 5879–5886.
66 J.-F. Paré, C. J. Martyniuk and M. Levin, Bioelectric regulation of innate immune system function in regenerating and intact *Xenopus laevis*, *Regen. Med.*, 2017, **2**, 15.
67 B. T. Chernet, D. S. Adams, M. Lobikin and M. Levin, Use of genetically encoded, light gated ion translocators to control tumorigenesis, *Oncotarget*, 2016, **7**, 19575–19588.

